

Phase Diagram of the Two-Dimensional Negative- U Hubbard Model

R. T. Scalettar

Department of Physics, University of Illinois, Urbana, Illinois 61801

E. Y. Loh and J. E. Gubernatis

Los Alamos National Laboratory, Los Alamos, New Mexico 87545

A. Moreo, S. R. White, D. J. Scalapino, and R. L. Sugar

Department of Physics, University of California, Santa Barbara, California 93106

E. Dagotto

Institute for Theoretical Physics, University of California, Santa Barbara, California 93106

(Received 16 January 1989)

Theoretical arguments and numerical calculations are used to discuss the phase diagram of the two-dimensional negative- U Hubbard model. Our results are consistent with (1) a vanishing transition temperature at half-filling but with a ground state having both superconducting and charge-density-wave long-range order, and (2) a Kosterlitz-Thouless transition at a finite temperature into a superconducting state with power-law decay of the pairing correlations away from half-filling.

PACS numbers: 75.10.Jm

The elimination of local phonon¹ or internal electronic² degrees of freedom can give rise to a short-range attractive interaction between the remaining electrons. Such a "negative- U " interaction leads to charge-density and pairing correlations. Here we investigate the phase diagram of the negative- U Hubbard model on a two-dimensional (2D) square lattice with

$$H = -t \sum_{\langle ij \rangle s} (c_{is}^\dagger c_{js} + c_{js}^\dagger c_{is}) - |U| \sum_i (n_{i\uparrow} - \frac{1}{2})(n_{i\downarrow} - \frac{1}{2}) - \mu \sum_{is} n_{is}, \quad (1)$$

where c_{is}^\dagger is an operator which creates an electron of spin s on the i th lattice site, t is a one-electron transfer integral, $|U|$ is the interaction strength, and the chemical potential μ determines the band filling. With the convention in Eq. (1), the half-filled band $\langle n \rangle = \langle n_{i\uparrow} + n_{i\downarrow} \rangle = 1$ has $\mu = 0$.

The physical properties of the negative- U Hubbard model depend upon $|U|/t$ and $\langle n \rangle$. For dimension $d \geq 3$, at half-filling there is a finite critical temperature separating a disordered phase from a low-temperature phase where charge-density-wave (CDW) order and superconductivity coexist.²⁻⁵ Away from half-filling the low-temperature phase is purely superconducting with a T_c which decreases with the filling. However, for $d=2$ we know that T_c at half-filling is zero. Does that imply that away from half-filling in the 2D model, T_c is also zero? Here we present theoretical arguments and results from numerical simulations and exact diagonalizations which suggest the type of phase diagram schematically illustrated in Fig. 1. In this figure the sections depict slices of a superconducting phase which has Kosterlitz-Thouless⁶ power-law pairing correlations. At half-filling,

$\langle n \rangle = 1$, the transition temperature is zero, but in the ground-state long-range CDW and pairing order coexist. Away from half-filling, the CDW correlations are short ranged. As discussed by Nozieres and Schmitt-Rink,⁷ the evolution from weak- to strong-coupling superconductivity appears to be continuous.

In the absence of the interaction U , the band structure $\epsilon_k = -2t(\cos k_x + \cos k_y)$ leads to a single-particle density of states which has a logarithmic Van Hove singularity at half-filling. In addition, the half-filled Fermi surface is perfectly nested for a momentum transfer of (π, π) . In weak coupling, these two features give rise to $\ln^2(t/T)$ singularities⁸ in both the pairing and the CDW channels and lead to a mean-field transition temperature $t \exp[-2\pi(t/|U|)^{1/2}]$. Away from half-filling, the characteristic energy for pairing varies as $(t\mu)^{1/2} \times \exp(-1/N(0)|U|)$, with $N(0) \sim (8t)^{-1}$, which is

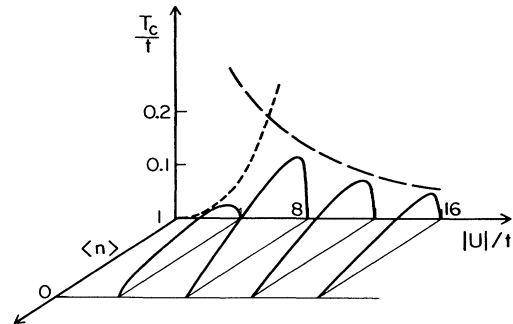


FIG. 1. Schematic T_c vs $|U|/t$ and $\langle n \rangle$ for the 2D negative- U Hubbard model. The short-dashed curve is the weak-coupling BCS prediction and the long-dashed curve is the strong-coupling energy $t^2/|U|$ divided by t .

shown as the short-dashed curve in Fig. 1. In the strong-coupling limit, the pair-binding energy is set by U and the pair transfer and near-neighbor repulsion are proportional to $t^2/|U|$, shown as the long-dashed curve in Fig. 1.

We will be interested in pairing and charge-density correlations described by $P = \langle \Delta^\dagger \Delta + \Delta \Delta^\dagger \rangle$ and $C(q) = \langle \rho_q \rho_q^\dagger \rangle$, where

$$\Delta^\dagger = \frac{1}{\sqrt{N}} \sum_l c_{l\uparrow}^\dagger c_{l\downarrow}^\dagger \quad (2)$$

and

$$\rho_q^\dagger = \frac{1}{\sqrt{N}} \sum_l e^{iq \cdot l} (c_{l\uparrow}^\dagger c_{l\uparrow} + c_{l\downarrow}^\dagger c_{l\downarrow}). \quad (3)$$

For half-filling, ρ_q^\dagger with $q = (\pi, \pi)$ corresponds to the operator for the CDW order parameter. Under the canonical transformation^{3,9,10} in which $c_{l\uparrow} \rightarrow c_{l\uparrow}$ and $c_{l\downarrow} \rightarrow (-1)^{l_x+l_y} c_{l\downarrow}^\dagger$, Eq. (1) becomes the Hamiltonian of a positive- U Hubbard model at half-filling in a uniform magnetic field $h = 2\mu$. The pair field operator Δ^\dagger becomes the transverse magnetic operator with $q = (\pi, \pi)$,

$$M_{x,y} = \frac{1}{\sqrt{N}} \sum_l (-1)^l c_{l\uparrow}^\dagger c_{l\downarrow}, \quad (4)$$

while $\rho_{(\pi,\pi)}^\dagger$ becomes the longitudinal staggered magnetization

$$M_z = \frac{1}{\sqrt{N}} \sum_l (-1)^l (n_{l\uparrow} - n_{l\downarrow}). \quad (5)$$

Now in the strong-coupling $|U|/t \gg 1$ limit, the half-filled positive- U Hubbard model maps onto an $s = \frac{1}{2}$ antiferromagnetic Heisenberg model with $J = 4t^2/|U|$. Thus in the strong-coupling limit, the original negative- U Hubbard model can be thought of in terms of the properties of a 2D Heisenberg model in an external magnetic field $h = 2\mu$,

$$H = J \sum_{\langle ij \rangle} \mathbf{S}_i \cdot \mathbf{S}_j - h \sum_i S_i^z. \quad (6)$$

Monte Carlo simulations of the Heisenberg model are consistent with a vanishing transition temperature and long-range isotropic antiferromagnetic correlations, with both transverse (pairing) and longitudinal (CDW) components, in the ground state.¹¹ Recent work on the 2D positive- U Hubbard model shows similar behavior for weak and strong coupling.^{12,13} Away from half-filling, the field h (or chemical potential μ) breaks the symmetry between transverse and longitudinal components and effectively makes the spins planar. In two dimensions, this distinction is crucial as it gives rise to a finite transition temperature. To see how an external magnetic field produces this effect, it is useful to consider a classical Heisenberg model. In the presence of h , the spins are forced to lie in the x - y plane but are canted toward the z axis with antiferromagnetic correlations in the x - y plane. In mean field, the canting angle θ out of the x - y plane is

set by $\sin\theta = h/8J$, corresponding in the negative- U Hubbard model to an occupation $\langle n \rangle = 1 - h/8J$. The effective xy exchange is

$$\begin{aligned} JS(S+1)\cos^2\theta &= JS(S+1)[1 - (h/8J)^2] \\ &= JS(S+1)\langle n \rangle(2 - \langle n \rangle). \end{aligned} \quad (7)$$

For a 2D classical xy model, this coupling would give rise to a Kosterlitz-Thouless transition⁶ with

$$T_c/J \sim \langle n \rangle(2 - \langle n \rangle). \quad (8)$$

In the negative- U Hubbard model, this corresponds to a transition to a superconducting phase with power-law decay $r^{-\eta}$ of the pairing correlations. Figure 2 shows the results of a Monte Carlo calculation of the power-law exponent of a classical 2D Heisenberg antiferromagnet in a uniform magnetic field with $h = J = 1$. We calculate η by comparing $\langle M_{xy}^2 \rangle \propto N^{1-\eta/2}$ on different sized lattices.¹⁴ Note the linear rise of η at low T , characteristic of the spin-wave behavior of correlations below T_c . Calculating η for different values of h/J and estimating T_c by the temperature where $\eta(T_c)$ takes the Kosterlitz-Thouless value⁶ $\eta = 0.25$, we obtain the points shown in the inset of Fig. 2. Near half-filling, when $h/J \ll 1$, a small-angle expansion about the canted state leads to an estimate of $J/|h|$ for the characteristic size of a vortex core. Determining T_c from the temperature at which this length becomes comparable to the 2D Heisenberg correlation length^{15,16} suggests that T_c goes to zero for $\langle n \rangle \rightarrow 1$ as

$$T_c/J \sim -2\pi/\ln(|1 - \langle n \rangle|), \quad (9)$$

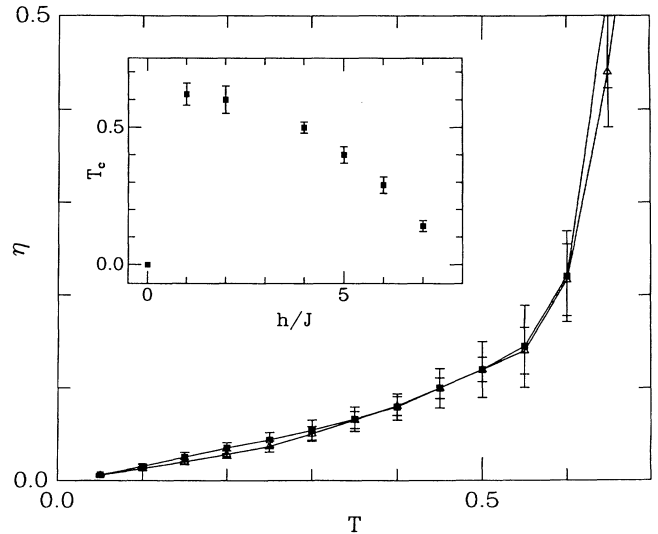


FIG. 2. η vs T for a classical Heisenberg model in an external magnetic field $h = J = 1$. The two curves were obtained by scaling (Ref. 14) 4×4 vs 16×16 lattices (Δ) and 8×8 vs 16×16 lattices (\blacksquare). Inset: T_c vs h obtained from plotting η vs T and taking T_c from the point at which $\eta = 0.25$ for different values of h .

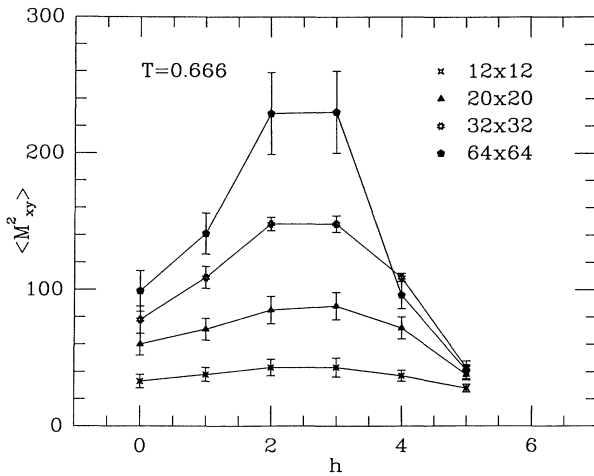


FIG. 3. The square of the staggered xy magnetization vs h at $T/J=0.66$ for various sized lattices for the classical Heisenberg model in an external field.

where $\langle n \rangle = 1 - h/8J$.

As further support of this picture, Fig. 3 shows Monte Carlo results for the square of the staggered xy magnetization

$$\langle M_{xy}^2 \rangle = \frac{1}{N} \left\langle \sum_{l,l'} (S_l^x S_{l'}^x + S_l^y S_{l'}^y) (-1)^{l+l'} \right\rangle \quad (10)$$

vs h for $T=0.66J$. Here one sees that as the lattice size increases, $\langle M_{xy}^2 \rangle$ appears to saturate for small and large values of h . However, for intermediate values of h , where according to Fig. 2 the system is near a Kosterlitz-Thouless phase, $\langle M_{xy}^2 \rangle$ increases with lattice size.

For the quantum problem, Fig. 4 shows results obtained on 4×4 lattices for the quantum $s = \frac{1}{2}$ model, and the negative- U Hubbard model with $|U|/t=8$. Here Lanczos exact-diagonalization procedure was used to calculate the ground-state expectation value of M_{xy}^2 for different values of S_z , the total z component of spin. Results for the negative- U Hubbard model were obtained using a recently developed Monte Carlo ground-state algorithm.¹³ From the plots one sees that these systems behave in a similar manner and lend support to the strong-coupling limit of the phase diagram of Fig. 1.

Further results for the negative- U Hubbard model are shown in Fig. 5. For the half-filled case, we expect^{12,13} that at $T=0$ there is long-range order in both the pair field and the CDW. If the asymptotic behavior is correctly described by spin-wave theory,¹⁷

$$P/N \approx |\langle \psi_0 | \Delta^\dagger | \psi_0 \rangle|^2 + A/N^{1/2} \quad (11)$$

for a lattice of N sites. Figure 5(a) shows a plot of P/N vs $N^{-1/2}$ for $\langle n \rangle = 1.0$ (\square), where P and C are equal, and $\langle n \rangle = 0.5$ for P (\blacksquare) and for C (\bullet). Here $U/t = -4$. (b) P and $C(\pi, \pi)$ vs β for different lattice sizes with $U/t = -4$ and $\langle n \rangle = 0.5$.

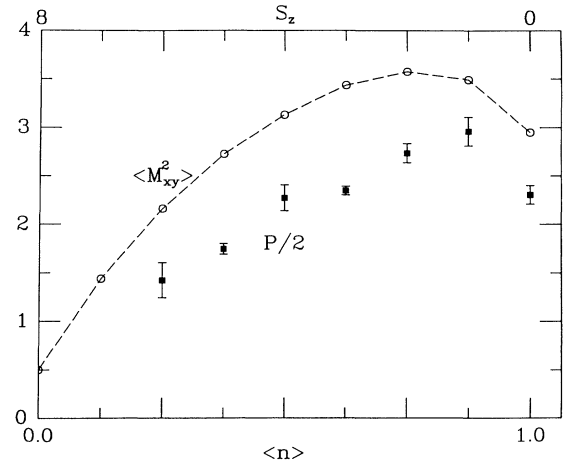


FIG. 4. The open circles show $\langle \psi_0 | M_{xy}^2 | \psi_0 \rangle$ vs the total z component of spin S_z (upper scale) for a quantum $s = \frac{1}{2}$ antiferromagnetic on a 4×4 lattice. The solid squares are ground-state Monte Carlo data for $P/2$ vs $\langle n \rangle$ for a Hubbard model on a 4×4 lattice with $|U|/t=8$.

seems to have long-range order. The CDW response has already saturated on the 4×4 lattice and does not change as the lattice size is increased, indicative of short-range CDW correlations.¹⁸ Figure 5(b) shows how P and

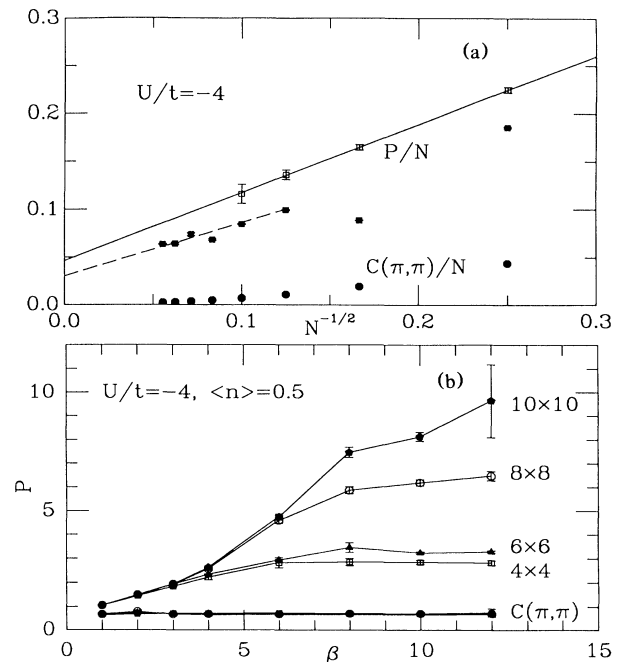


FIG. 5. (a) Pair field P and CDW structure factor $C(\pi, \pi)$ vs $N^{-1/2}$ for $\langle n \rangle = 1.0$ (\square), where P and C are equal, and $\langle n \rangle = 0.5$ for P (\blacksquare) and for C (\bullet). Here $U/t = -4$. (b) P and $C(\pi, \pi)$ vs β for different lattice sizes with $U/t = -4$ and $\langle n \rangle = 0.5$.

$C(\pi, \pi)$ vary with temperature and lattice size at filling $\langle n \rangle = 0.5$. Clearly the CDW correlations are suppressed while the superconducting correlations grow with both lattice size and inverse temperature.

Here we have argued that doping away from half-filling leads to a finite superconducting T_c for the 2D negative- U Hubbard model. Clearly, other mechanisms can also accomplish this. For example, at half-filling a near-neighbor attractive interaction V leads in strong coupling to a superconducting transition for $0 < |V| < 2t^2/|U|$ and phase separation for $|V| > 2t^2/|U|$. Other interactions, such as a next-near-neighbor hopping can also favor superconductivity.⁸ However, the Hubbard model discussed here provides a particularly simple example which also has interesting consequences for quantum field theory. The classical Heisenberg model in 2D [the O(3) model] has $T_c = 0$ because it is asymptotically free.¹⁹ Figure 1 suggests that this property disappears in the presence of a staggered magnetic field.

We would like to acknowledge useful discussions with J. Cardy and S. Chakravarty. This work was supported in part by the Department of Energy under Grant No. DE-FG03-88ER45197 and the National Science Foundation under Grants No. PHY87-01775 and No. PHY82-17853 and was supplemented by funds from NASA and by the San Diego Supercomputer Center. S.R.W. gratefully acknowledges the financial support of IBM. The numerical work reported in this paper was done on the Cray-XMP at the San Diego Supercomputer Center.

¹P. W. Anderson, Phys. Rev. Lett. **34**, 953 (1975).

²J. E. Hirsch and D. J. Scalapino, Phys. Rev. B **32**, 5639 (1985).

³S. Robaszkiewicz, R. Micnas, and K. A. Chao, Phys. Rev. B **23**, 1447 (1981); **24**, 1579 (1981).

⁴As a result of the recently found connection between Hubbard models and lattice gauge theories [E. Dagotto, E. Fradkin, and A. Moreo, Phys. Rev. B **38**, 2926 (1988)], the phase diagram of the $U < 0$ Hubbard model for $d=3$ was also obtained in E. Dagotto, A. Moreo, and U. Wolff, Phys. Lett. B **186**, 395 (1987).

⁵C. M. Varma, Phys. Rev. Lett. **61**, 2713 (1988).

⁶J. M. Kosterlitz and D. J. Thouless, J. Phys. C **6**, 1181 (1973).

⁷P. Nozieres and S. Schmitt-Rink, J. Low Temp. Phys. **59**, 195 (1985).

⁸J. E. Hirsch and D. J. Scalapino, Phys. Rev. Lett. **56**, 2732 (1986).

⁹H. Shiba, Prog. Theor. Phys. **48**, 2171 (1972).

¹⁰V. J. Emery, Phys. Rev. B **14**, 2989 (1976).

¹¹J. D. Reger and A. P. Young, Phys. Rev. B **37**, 5978 (1988).

¹²J. E. Hirsch and S. Tang, University of California, San Diego, report, 1988 (to be published).

¹³S. R. White, D. J. Scalapino, R. L. Sugar, E. Y. Loh, J. E. Gubernatis, and R. L. Scalettar, University of California, Santa Barbara, Report No. UCSBTH-88-18 (to be published).

¹⁴Here $\langle M_{xy}^2 \rangle_{N,T}$ is calculated at a temperature T on an N -site lattice. Then using two different sized lattices N and N' , one has

$$\eta(T) = 2[1 - \ln(\langle M_{xy}^2 \rangle_{N,T} / \langle M_{xy}^2 \rangle_{N',T}) / \ln(N'/N)].$$

¹⁵S. Hikami and T. Tsuneto, Prog. Theor. Phys. **63**, 387 (1980).

¹⁶This is of course a classical estimate for the strong-coupling limit. For the $s = \frac{1}{2}$ problem, quantum fluctuations reduce the factor of 2π in Eq. (9) by a renormalization factor of order 0.25. Furthermore, in the Hubbard model, charge fluctuations give $\langle (n_{l1} - n_{l2})^2 \rangle < 1$, further reducing T_c .

¹⁷D. A. Huse, Phys. Rev. B **37**, 2380 (1988).

¹⁸We have examined the structure factor $\langle \rho_q^\dagger \rho_q \rangle$, and although the peak moves away from $q = (\pi, \pi)$, its behavior with lattice size is similar to the results shown in Fig. 5.

¹⁹A. Polyakov, Phys. Lett. **59B**, 79 (1975).